Proceedings of ICRC 2001: 63 © Copernicus Gesellschaft 2001

ICRC 2001

The primary energy spectrum of cosmic rays obtained by muon density measurements at KASCADE

A. Haungs[1], T. Antoni[1], W. D. Apel[1], F. Badea[2], K. Bekk[1], A. Bercuci[1,2], K. Bernlöhr[1,*], H. Blümer[1,3], E. Bollmann[1], H. Bozdog[2], I. M. Brancus[2], C. Büttner[1], A. Chilingarian[4], K. Daumiller[3], P. Doll[1], J. Engler[1], F. Feßler[1], H. J. Gils[1], R. Glasstetter[3], R. Haeusler[1], D. Heck[1], J. R. Hörandel[3], T. Holst[1], A. Iwan[5,3], K-H. Kampert[1,3], J. Kempa[5,+], H. O. Klages[1], J. Knapp[3,¶], G. Maier[1], H. J. Mathes[1], H. J. Mayer[1], J. Milke[1], M. Müller[1], R. Obenland[1], J. Oehlschläger[1], M. Petcu[2], H. Rebel[1], M. Risse[1], M. Roth[1], G. Schatz[1], H. Schieler[1], J. Scholz[1], S. H. Sokhoyan[4], T. Thouw[1], H. Ulrich[3], B. Vulpescu[2], J. H. Weber[3], J. Wentz[1], J. Wochele[1], J. Zabierowski[6], and S. Zagromski[1]

[1]Institut für Kernphysik, Forschungszentrum Karlsruhe, 76021 Karlsruhe, Germany
[2]National Institute of Physics and Nuclear Engineering, 7690 Bucharest, Romania
[3]Institut für Experimentelle Kernphysik, University of Karlsruhe, 76021 Karlsruhe, Germany
[4]Cosmic Ray Division, Yerevan Physics Institute, Yerevan 36, Armenia
[5]Department of Experimental Physics, University of Lodz, 90236 Lodz, Poland
[6]Soltan Institute for Nuclear Studies, 90950 Lodz, Poland
[*]now at: Humboldt University, Berlin, Germany
[+]now at: Warsaw University of Technology, 09-400 Plock, Poland
[¶]now at: University of Leeds, Leeds LS2 9JT, U.K.

Abstract. Spectra of local muon densities in high-energy extensive air-showers (EAS) are presented as signature of the primary cosmic ray energy spectrum in the knee region. The KASCADE central detector, with its two layers of multiwire proportional chambers and with a layer of scintillation counters, enables the measurements of muon densities at two different threshold energies. The spectra have been reconstructed for various core distances, as well as for particular subsamples, classified on the basis of the shower size ratio N_μ/N_e. The measured density spectra of the total sample exhibit clear kinks reflecting the knee of the primary energy spectrum. While relatively sharp changes of the slopes are observed in the spectrum of EAS with small values of the shower size ratio, no such feature is detected at EAS of large N_μ/N_e ratio in the energy range of 1–10 PeV. In addition to these findings the validity of EAS simulations is studied by comparing the spectra for different muon energy detection thresholds and core distances with detailed Monte Carlo simulations. No consistent energy spectrum can be derived from the data for the two muon thresholds, irrespective of assumptions on elemental composition.

1 Introduction

Though the first evidence of the existence of the knee in the primary cosmic ray energy spectrum has been presented more than 40 years ago, the knowledge of the detailed structure of the spectrum in the PeV region is still scarce, and the origin of the knee not yet understood. Frequency spectra of the observables of the necessarily indirect measurements (like number of electrons or charged particles) reflect in principle the primary energy spectrum, but a quantitative conversion to energy has to invoke a model of the shower development and on an assumption of a mass composition. Hence the determination of the energy spectrum is affected by different systematic uncertainties, especially by the dependence on the model of high-energy interactions. This also leads to a mutual dependence of the results for the energy spectrum and mass composition. It would be useful to analyze different experiments on basis of a coherent methodology as well as to compare the resulting features for various sets of different EAS parameters in the individual experiments.

In the present paper we endeavor to analyze the frequency distribution of local muon densities at fixed distances from the shower core. While the reconstruction of electron or muon size spectra necessarily implies a choice of the form of the lateral distribution function, spectra of the muon density are free from this bias. Thus independent measurements of such spectra for different fixed core distances allow a check on the lateral distribution obtained from simulations. In addition, the layout of the KASCADE experiment (Klages et al., 1997), enables the study of density spectra for two different muon energy thresholds. Hence the consistency of the simulations with respect to the muon energy spectrum can be performed.

Correspondence to: A. Haungs (haungs@ik3.fzk.de)

2 Reconstruction of local muon densities

The main detector components of KASCADE used for the present analysis are an “array” of 252 stations and a “central detector” comprising additional detector systems. The array provides the data necessary for the reconstruction of the basic EAS characteristics like electron and muon size, core location, and arrival direction of individual air showers. The special arrangement of shielded and unshielded detectors on top of each other allows an independent estimation of the electron and muon number for each individual shower (Antoni et al., 2000). The KASCADE central detector is placed at the geometrical center of the detector array. It consists of four different detector systems, covering a total area of $16\times20\,\mathrm{m}^2$. The local muon density of EAS is measured with the multiwire proportional chambers (MWPC) and the trigger plane. A setup of 32 large multiwire proportional chambers is installed (Bozdog et al., 2001) in the basement of the building. The total absorber corresponds to a threshold for vertical muons of 2.4 GeV. Only that area where muons parallel to the shower axis would penetrate the whole absorber and both chamber planes, is taken into account for the calculation of the muon density. This local muon density $\rho_\mu^\star$ is defined by the number of tracked muons $N_\mu^\star$ divided by the total sensitive area $A^\star$ of the MWPC setup. Due to the layout of the chambers, $A^\star$ depends on the angle of incidence of the shower and is calculated for each event individually ($\langle A^\star\rangle = 107\,\mathrm{m}^2$ for the selected EAS).
The second muon detection system is a layer of 456 plastic scintillation detectors in the third gap of the central detector, called trigger plane (Engler et al., 1999). The muon density ρ_μ^{tp} (with a threshold of 490 MeV for vertical incidence) is reconstructed in the following way: To remove signals from cascading hadrons in the absorber an upper limit of the energy deposit of 30 MeV in each of the 456 scintillation counters is imposed. Detectors with larger energy deposits and their immediate neighbours are not considered for further reconstruction. For the remaining detectors, the energy deposit and the sensitive area, both corrected for the shower direction, are summed up. The number of reconstructed muons N_μ^{tp} is then calculated by the sum of the energy deposits divided by the mean energy deposit of a single muon in the shower, according to Monte Carlo calculations. The density ρ_μ^{tp} is obtained as ratio of N_μ^{tp} and the sensitive area of the trigger plane for each individual event ($\langle A^{\mathrm{tp}}\rangle = 202\,\mathrm{m}^2$).
The core distances R_c of the local densities $\rho_\mu^\star$ and ρ_μ^{tp} are estimated in a plane perpendicular to the shower axis.

3 Local muon density spectra

The reconstruction of muon density spectra have been performed for two energy thresholds and for nine core distance ranges (Figs. 1 and 2). To suppress punch-through effects of the hadronic or electromagnetic component, EAS with $R_\mathrm{c} < 30\,\mathrm{m}$ are excluded. EAS with $R_\mathrm{c} > 72\,\mathrm{m}$ are excluded, too, because they can have their core outside of the fiducial area of the KASCADE array if they are very inclined. Fig. 1 and Fig. 2 show the flux spectra for the two muon thresholds in integral form. The flux values are multiplied by $(\rho_\mu^\star)^{2.3}$ and $(\rho_\mu^{\mathrm{tp}})^{2.0}$, respectively. All spectra show a slight, but significant kink with decreasing density for increasing core distance. For the fit procedure the flux $lg(\frac{dN}{d\rho_\mu})$ is assumed to follow a power law below and above a specified knee region. The fit procedure estimates the indices of these power laws, the position of the knee (if existing), and the boundaries of the different regions. The position of the knee is calculated as the weighted center of gravity of the bins inside the knee region. The “width” of the knee region for all spectra amounts to $\Delta lg(\rho_\mu/\mathrm{m}^{-2}) \approx 0.15$. The higher muon energy threshold results in steeper spectra. This indicates a comparatively larger increase of the muon density per primary energy interval with increasing muon energy threshold. The spectra for different core distances are almost parallel leading to nearly constant indices for a given muon energy threshold. This confirms previous experimental results (Antoni et al., 2001) of only slight changes of the shape of the muon lateral distributions with increasing primary energy (which is different for the electromagnetic component of EAS). For both energy thresholds there is a clear difference in the indices below and above the knee.

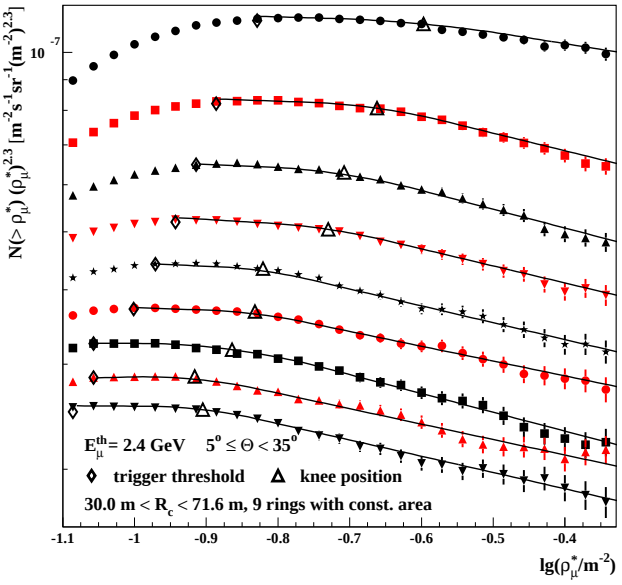

Fig. 1. Integral spectra of the local muon density $\rho_\mu^\star$ as measured by the MWPC system for different core distances R_c (from top to bottom with increasing R_c). The upper limits of the radial bins are 37.0, 42.9, 48.0, 52.7, 57.0, 60.9, 64.7, 68.2, and 71.6 m, respectively. The lines represent the results of the fit procedure.

The total sample of EAS as displayed in Figs. 2,3 is further on separated in “electron-rich” and “electron-poor” showers performed by a cut in the ratio $lg(N'_\mu)/lg(N'_e)$ (at a value of 0.75, optimized by Monte Carlo calculations). The measured shower sizes are converted to the sizes of vertical show-

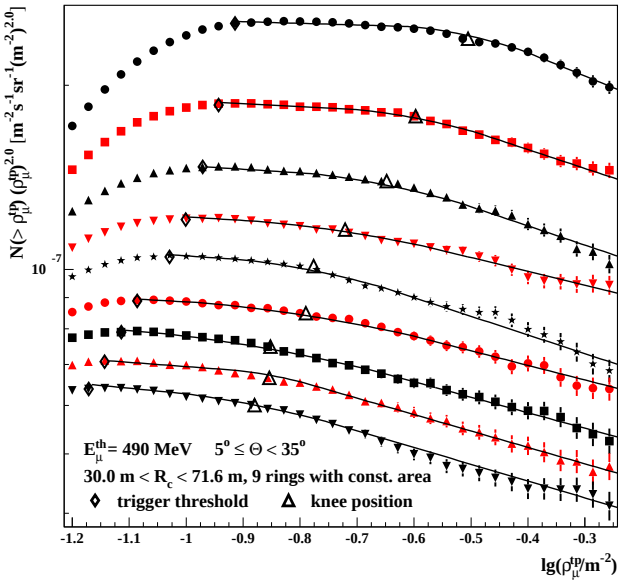

Fig. 2. Same as Fig. 1 but for the local muon density $\rho_\mu^{\rm tp}$ measured by the trigger plane.

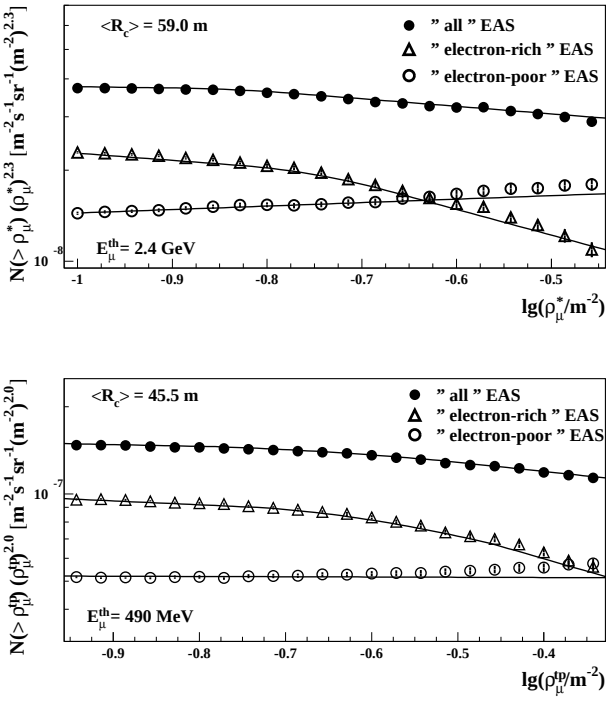

Fig. 3. Examples for measured spectra of different muon content. The "all"-particle spectra have already been shown in Figs. 1 and 2 and are here compared with the spectra of "electron-poor" and "electron-rich" EAS for the same core distance range.

ers to eliminate the influence of the different zenith angles:
$ln(N_e') = ln(N_e) - \frac{X}{\Lambda_e} \cdot (\sec\theta - 1)$
$ln(N_\mu') = ln(N_\mu^{\rm tr}) - \frac{X}{\Lambda_\mu} \cdot (\sec\theta - 1)$
where N_e, $N_\mu^{\rm tr}$, and θ are the reconstructed quantities of the EAS, and $X = 1022\,{\rm g/cm^2}$ is the depth of the observation level. The quantities Λ_e and Λ_μ denote the absorption lengths of the electron and muon components in the atmosphere. The values were obtained from Monte Carlo simulations and parameterised as $\Lambda_e = 104.3 + 13.5 \cdot lg(N_e)\,{\rm g/cm^2}$ and $\Lambda_\mu = 5 \cdot \Lambda_e$. Especially the electron number depends significantly on the zenith angle due to the rapidly increasing atmospheric absorption. The cut value is optimized by Monte Carlo calculations. For both subsamples the spectra are deduced in the same way as the "all-particle" spectra.
As example Fig. 3 shows the reconstructed local muon density spectra for $\langle R_{\rm c}\rangle = 45.5\,{\rm m}$ for the lower muon energy threshold and for $\langle R_{\rm c}\rangle = 59.0\,{\rm m}$ for the higher threshold. Spectra for all, for the electron-rich (predominantly light ion induced), and for the electron-poor (predominantly heavy ion induced) showers are displayed. The general features of the spectra are similar for all core distance ranges; the component of electron-rich EAS dominates the flux below the knee while it strongly decreases after the kink. No knee is seen in the component of electron-poor EAS. The resulting slopes of the spectra, especially the differences of the slope-values for the two thresholds and subsamples, are very similar for the various core distances. Whereas the assumed fit functions describe the all-particle spectra well, the spectra for the EAS subsamples are not well described by power laws above the densities of the knee at the all-particle spectra.

4 Comparisons with simulations

For the interpretation of the measured muon density spectra in terms of the primary energy spectrum a-priori knowledge inferred from Monte Carlo simulations of the air-shower development is necessary. The present analysis is based on a large set of CORSIKA (v 5.62) simulations (Heck et al., 1998) including a full simulation of the detector response. The simulations have been performed using the interaction model QGSJET (Kalmykov et al., 1997) for the high-energy interactions and GHEISHA (Fesefeldt 1985) for interactions below $E_{\rm lab} = 80\,{\rm GeV}$ and subsequent decays. The electromagnetic part of the showers is treated by EGS4 (Nelson et al., 1985). Observation level, earth's magnetic field, and the particle thresholds are chosen in accordance with the experimental situation of KASCADE. The simulations cover the energy range of $5 \cdot 10^{14} - 3.06 \cdot 10^{16}\,{\rm eV}$. The calculations are performed for three zenith angular ranges ($0° - 15°$, $15° - 20°$, $20° - 40°$) and for three primary masses: protons, oxygen and iron nuclei. The output of the simulations is analyzed by the same procedures as applied to the measured data, reducing systematic uncertainties.

When relating the density spectra to the primary energy spectrum of cosmic rays a power law spectrum $dN\,/\,dE_0 \propto E_0^{-\gamma}$ is assumed. The energy spectrum can be written as $dN\,/\,d\rho_\mu \cdot d\rho_\mu\,/\,dE_0$, where $d\rho_\mu\,/\,dE_0$ has to be deduced from the EAS simulations and $dN\,/\,d\rho_\mu \propto (\rho_\mu)^{-\beta}$ is taken

from the experimental results. Thus the spectral index γ can be expressed by $\gamma = \delta \cdot (\beta - 1) + 1$ with δ from the simulations ($\rho_\mu \propto {E_0}^\delta$). It could be shown (Antoni et al., 2001a) that this assumption of a power law is valid for all primary masses, all core distance ranges and both muon energy thresholds, whereas the value of δ certainly varies. If the correct elemental composition is adopted, all measured muon density spectra (of the total sample or of a certain subsample) should result consistently in the true primary energy spectrum, irrespective which core distance and muon energy threshold are considered.

The muon density spectra for the different core distances agree within their statistical uncertainties for the resulting slopes and knee positions of the primary mass (Antoni et al., 2001a). This supports the confidence in the lateral distribution predicted by the Monte Carlo simulations. Nevertheless there remain obvious systematic differences in the results for the two muon energy thresholds, observed for all core distances. The systematic differences might arise from possibly incorrect assumptions on mass composition due to the sensitivity of the muon spectrum to primary mass. Such an effect, however, should be considerably reduced when analysing the electron-rich and electron-poor subsamples which should be enriched in light and heavy primaries, respectively. But the systematic differences for the two thresholds remain. Uncertainties by the unknown composition can not explain the systematic discrepancy displayed by the results from the two different muon energy thresholds. Therefore we conclude that an incorrect description of the muon energy spectrum by the Monte Carlo simulations is the origin of the discrepancy. The effect does not only occur for the QGSJet model used for the present analysis. A smaller sample of reference showers generated with the VENUS (Werner 1993) model has been used to study the observed difference. A general shift to a steeper primary energy spectrum ($\Delta\gamma \approx 0.2$) and a lower knee position is found. This can be explained by the differences in the muon energy spectrum (Fig. 4) caused by the high-energy interaction model (see also Antoni et al., 2001b). The larger number of produced muons will modify the density to primary energy relation in the observed way. However, the inconsistency with respect to the two different muon energy thresholds persists. The considered muon energies are comparatively low, and are treated in the CORSIKA simulation code mainly by the low-energy interaction model GHEISHA. Thus the inconsistencies are most probably due to the low-energy model. Fig. 4 shows the muon energy spectrum also for the case of simulated EAS with QGSJET as high-energy model and the UrQMD (Bass et al., 1998) program as generator of the low energy interactions and the decays. Here an primary energy and muon threshold dependent change of the muon numbers is observed, which will lead to a more consistent description of the measurements.

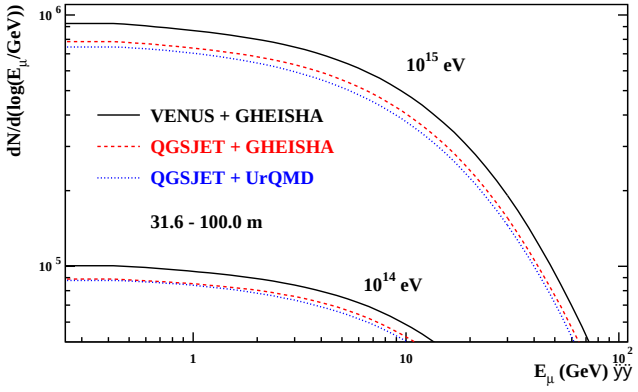

Fig. 4. Mean muon energy spectra for vertical proton induced showers of fixed energies, generated with different high-energy and low-energy interaction models. The spectra are displayed for the radial range of interest and in integral form.

5 Conclusions

In view of the systematic discrepancies related with the measure for two muon energy thresholds, it is difficult to draw definite conclusions but some general features of the primary energy spectrum can be stated: The all-particle energy spectrum exhibits a knee at $E_{\mathrm{knee}} \approx (3-5) \cdot 10^{15}$ eV with a change of the spectral index of order $\Delta\gamma \approx 0.2 - 0.3$. This knee is only seen in the light ion subsample, at the same position but with a distinctly larger steepening of $\Delta\gamma \approx 0.5$. The heavy ion component of the cosmic ray flux displays no steepening in the energy range of 1–10 PeV and a smaller slope than the light component below the knee.

Acknowledgements. The KASCADE experiment is supported by Forschungszentrum Karlsruhe and by collaborative WTZ projects in the frame of the scientific-technical cooperation between Germany and Romania (RUM 97/014), Poland (POL 99/005) and Armenia (ARM 98/002). The Polish group (Soltan Intitute and University of Lodz) acknowledges the support by the Polish State Committee for Scientific Research (grant No. 5 P03B 133 20).

References

Antoni, T., et al. - KASCADE collaboration, Astrop.Phys., 14, 245, 2001.
Antoni, T., et al. - KASCADE collaboration, Astrop.Phys., 2001a, in press; astro-ph/0103363.
Antoni, T., et al. - KASCADE collaboration, Astrop.Phys., 2001b, in press; astro-ph/0102443.
Bass, S.A., et al., Prog. Part. Nucl. Phys., 41, 225, 1998.
Bozdog, H., et al., NIM A, 2001, in press.
Engler, J., et al., NIM A, 427, 528, 1999.
Fesefeldt, H., PITHA-85/02, RWTH Aachen, 1985.
Heck, D., et al., FZKA 6019, Forschungszentrum Karlsruhe, 1998.
Kalmykov, N., et al., Nucl. Phys. B (Proc. Suppl.), 52B, 17, 1997.
Klages, H.O., et al., Nucl. Phys. B, Proc. Suppl., 52B, 92, 1997.
Nelson, W.R., et al., SLAC 265, Stanford Linear Accelerator, 1985.
Werner, K., Phys. Rep., 232, 87, 1993.